5-2022

Experimental Study of Moisture Effect on the Nanofiber Z-Threaded Carbon Fiber Reinforced Polymer Prepreg and Its Composite

Md Nazim Uddin
University of South Alabama, mu1621@jagmail.southalabama.edu

EXPERIMENTAL STUDY OF MOISTURE EFFECT ON THE NANOFIBER Z-THREADED CARBON FIBER REINFORCED POLYMER PREPREG AND ITS COMPOSITE

A Thesis

Submitted to the Graduate Faculty of the
University of South Alabama
in partial fulfillment of the
requirements for the degree of

Master of Science

in

Mechanical Engineering

by
Md Nazim Uddin
BSME, University of South Alabama, 2020
May 2022

ACKNOWLEDGMENTS

I thank my graduate research mentor Dr. Hsiao for enlisting me in his research group and for the unique guidance during my research in his composite lab. Which gave me the opportunity to enhance my analytical and experimental skills related to composite manufacturing. I thank Dr. Richardson for his warm-hearted welcoming approach during my undergraduate and graduate studies here at the University of South Alabama. Finally, thank you Dr. Latif for his advice, guidance, and being on my thesis defense committee.

I also thank my co-workers in the Hsiao Group for their kind support and assistance. Especially, I appreciate the help of Wyatt Taylor, Mohammad Rakibul Islam, and Mason Brasher in preparing the composite testing samples for the experiments.

This thesis research performed at the Hsiao Group has been under the financial support of the National Science Foundation (Award number: 2044513), Alabama Department of Commerce through the Alabama Innovation Fund (Award number: 150436). The carbons fiber materials provided by Hexcel, the surfactants provided by BYK USA, Inc. are also acknowledged.

TABLE OF CONTENTS

Page

LIST OF TABLES

LIST OF FIGURES

LIST OF ABBREVIATIONS

CNFs = Carbon nanofibers

ZT-CFRP = Z-threaded carbon fiber reinforced polymer

ILSS = Interlaminar shear strength

CFRP = Carbon fiber reinforced polymer

OOA-VBO = Out of autoclave- vacuum bag only

CF = Carbon fiber

FVF = Fiber volume fraction

SBS = Short beam shear

DNS = Double notch shear

SCF = Short carbon fiber

COV = Coefficient of variance

RH = Relative humidity

3D = Three dimensional

ABSTRACT

Uddin, Md, Nazim, M.S., University of South Alabama, May 2022. Experimental study of moisture effect on the nanofiber Z-threaded carbon fiber reinforced polymer prepreg and its composite. Chair of Committee: Dr. Kuang-Ting Hsiao, Ph.D

A persistent issue found in Carbon Fiber Reinforced Polymer (CFRP) manufacturing is moisture contamination. During manufacturing, this issue is present when a CFRP prepreg is carefully thawed, cut, stacked, and cured into the desired laminate. The moisture affects the structural integrity of the finished laminate and can present as voids. Recent advancements in carbon nanofiber (CNF) z-threaded CFRP (i.e., ZT-CFRP) prepreg have yielded laminates that have significant multifunctional improvements in, but are not limited to, mechanical strength, toughness, thermal conductivity, and electrical conductivity. This approach affects the microstructure of the laminate in which the CNF interlocks with the carbon fiber along the through-thickness direction (i.e., Z-direction) giving an effective 3D-fiber-network reinforced laminate. In this study, the impact of relative humidity (RH) on the interlaminar shear strength (ILSS) and the hardness of ZT-CFRP and traditional CFRP prepregs during handling and lamination processes are investigated. The microscopic analysis will aid in explaining how different moisture conditions affect the sample laminates. ILLS testing provides a glimpse into how the different moisture conditions affect the ZT-CFRP and the CFRP laminates.

CHAPTER I

INTRODUCTION

The void created by moisture content during the carbon reinforced polymer (CFRP) composite manufacturing has been a concern for years due to their disagreeable influence on mechanical properties [1] such as the interlaminar shear strength (ILSS). The interlaminar shear strength can be reduced from 17 Ksi to 8 Ksi if there is approximately 8% void in the epoxy-based CFRP with fiber volume fraction of 60%-70% [1]. Void formation in a CFRP laminate is commonly caused by the air, volatiles, and moisture entrapped in the prepreg prior to the curing process. The moisture in the fiber-epoxy system can further influence the degree of cure, void formation, and mechanical properties. Sharp et al. [2] reported that the water in an epoxy resin system can influence the cure rate; specifically, the water absorption increases the cure rate at the low degree of cure and decreases the cure rate at the high degree of cure. It is because the water-infused epoxy system has a higher cure rate initially due to the molecular self-diffusion of the epoxy molecule. However, with the increase of water content in an epoxy system, the water molecules are pushed by the cured epoxy to form water pockets that limit the full curing of the nearby epoxy eventually. They also found that low fraction of water content (0.5%) caused the plasticization of the resin and increased the fracture toughness. However, a higher water content (2%) reduced the fracture toughness by 20%. Nogueira et al. [3]

reported that, as the water content in an epoxy system was increased from 0 to 1.9%, the tensile modulus increased from 1500 MPa to 1560 MPa and the strength was reduced from 64 MPa to 54 MPa. Flexure mechanical properties of epoxy adhesive in the presence of different level of RH/water have been examined by Lettieri and Frigione [4] where the epoxy adhesive was exposed to RH-55%, RH-75%, and RH-100% environments for a range from zero to 28 days. Their flexural strength test data maximized at either 12 days or 28 days of exposure to moisture with higher standard deviation among the samples. Based on the aforementioned reports, one can conclude that the moisture effects in CFRP manufacturing can be quite complex from the views of resin curing enhancement, resin mechanical properties, and voids.

The recent advance in nanocomposites, especially the use of carbon nanofibers in CFRP has shown promising potential in enhancing the CFRP's mode-I delamination toughness [5], interlaminar shear strength [6], z-directional electrical conductivity [7], and z-directional thermal conductivity [8]. The carbon nanofibers zig-zag threaded through the carbon fiber bed/plies in the thickness direction (i.e., z-threading) of a CFRP prepreg (i.e., ZT-CFRP prepreg) and provided the additional interlaminar, intralaminar reinforcement and the z-directional conductive path in a CFRP laminate. In this preliminary study, it is hypothesized that the ZT-CFRP prepreg could also improve CFRP laminate manufacturing with respect to the moisture exposure concern. The ZT-CFRP prepreg will be exposed to moisture prior to being stacked and cured into a ZT-CFRP laminate. The ILSS and the hardness of the laminate samples made of regular CFRP and ZT-CFRP prepregs, with and without RH exposure prior to the curing process, will be tested and compared.

1.1 Literature Review

1.1.1 Carbon Fiber Reinforced Polymer laminates advancement in current industry

Demand for carbon fiber reinforced polymers has been expanding exponentially in the electric vehicle (EV), aerospace, and sports industries due to their superior mechanical performance which comes from their improved strength to weight ratio compared to traditional metals and alloys. Automotive manufacturers discovered cars made from CFRP and alloys could be half the weight of cars made with traditional metals [9]. Similarly, aerospace industries have been using CFRP heavily in their structure take advantage of this ratio. The world renown aircraft manufacturer Boeing made the 787 Dreamliner carrier which consists of almost 50 percent of CFRP in its structure. Another aircraft manufacturer implementing this technology is Airbus and its A380 aircraft, currently in the largest aircraft carrier in the world, used almost 25 percent of CFRP on its construction [10]. The sports composite market predicts to grow up to 4.58 billion dollars by 2024[11]. In 2015 alone, the golf club industry contributed 38% of the total market revenue. The industries listed above are still increasing the portion of CFRP used in their application. However, due to the weakness (matrix-dominated properties) in the traditional CFRP, adaptation has been challenging. To overcome those challenges, researchers have been studying nanoparticles (carbon nanofiber (CNF), and carbon nanotube (CNT)) for decades. The addition of CNFs and CNTs further reinforce CFRP in the through-thickness direction and enhance CFRP laminate's mechanical, electrical, and thermal properties. This trend of using CNFs and CNTs has become more common due to the better dispersion processes

and affordable prices. The CFRP laminates morphology changes due to the addition of CNFs and CNTs and the fracture behavior of laminates enlightens researchers on how best to position them in CFRP laminates. Studies have shown that through-thickness reinforcement of CNFs or CNTs further enhanced the CFRP's mechanical and electrical properties [12] compared with other reinforcement techniques. The through-thickness nano-reinforcement technology of using CNFs and CNTs developed by the Hsiao group [12] is known as the ZT-CFRP composite, which stands for carbon nanofibers/carbon nanotubes "z-threaded" CFRP, enabling to the enhancement of traditional CFRP materials interlaminar shear strength (ILSS) as much as 17%, electrical conductivity (Z-direction) as much as 1508%, and thermal conductivity (Z-direction) 6531%.[12]. These mechanical, electrical, and thermal properties enhanced by this patented ZT-CFRP technology (US8451013B1, US10556390B2, US10947356B2) have been recognized by sports and automotive industries and the Hsiao group is working on scaling the production line and feasibility for a start-up in coming years.

1.1.2 Moisture and quality of CFRP laminates

The scaling of production from laboratory to industrial level comes with many challenges. Moisture contamination plays a significant role in the final CFRP laminates quality. Moisture has a direct relationship with the void formation in final laminate's regardless of its origin in the CFRP manufacturing process. The void formation in CFRP mainly comes from three sources in the manufacturing processes: air entrapment, presence of volatiles in the raw materials used in the manufacturing process, and moisture entrapped in the prepreg prior to the curing process [13]. The void fraction in the final prepreg has an

inverse relationship with mechanical, electrical, and thermal properties. The increase in void content, disregarding the reasons for void formation, gradually diminishes the ILSS in the final CFRP laminates illustrated in Figure 1 [1]. Researchers are working to eradicate moisture from resin blends to produce quality CFRP products. In so Doing, Researchers and industries have introduced processes in manufacturing in the past which are outdated and result in time-consuming, complicated, and inflexible methods like autoclave and out-of-autoclave vacuum bag only (OOA-VBO) curing processes as lowering the moisture content at the source has always been challenging. In addition to the traditional methods, the advancement of manufacturing processes like additive manufacturing (3D printing) are also very sensitive to moisture control and in many situations the feedstocks of the 3D printing process are recommended to be stored in a dry environment to prevent moisture effects caused by weaker parts. The eradication of moisture at the source (pre-curing stages) in CFRP manufacturing is possible following more advances in quality control.

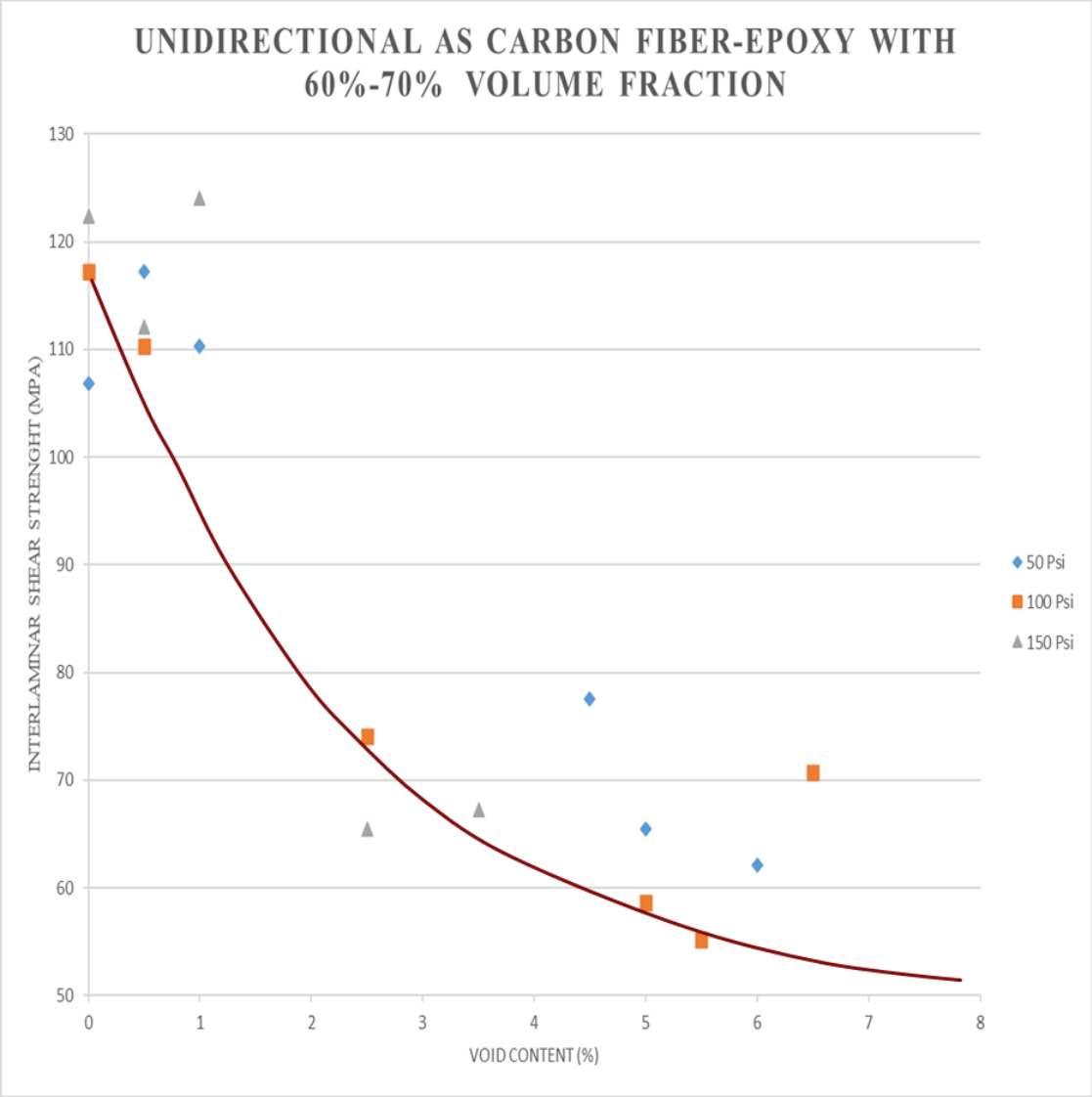

Figure 1. Effect of void volume fraction on the interlaminar shear strength of composite laminate (redrawn from [1])

CHAPTER II

OBJECTIVE AND METHODS

This chapter will address the materials used to manufactured control CFRP, ZT-CFRP prepreg and laminates along with ZT-Film manufacturing, prepreg manufacturing, prepreg exposure to outdoor RH, quality control, and curing methods.

2.1 Materials

To understand the influence of moisture on regular CFRP and ZT-CFRP prepregs, five type of laminate samples were manufactured for the double notch shear (DNS) ILSS test. Two laminate samples were manufactured from the traditional CFRP prepregs, in which one of their prepreg sets (two 10-inch x 20-inch prepregs to make a 20-ply CFRP laminate) was exposed to RH (to be described in detail in Section 2.2) as mentioned in graph 2 for approximately 24 hours before being processed into a CFRP laminate. The two large prepregs were trimmed into 20 pieces and the 20 plies were stacked up on top of an aluminum mold. The assembly of prepreg-stack was cured into a rigid CFRP laminate using the out of autoclave-vacuum bag only (OOA-VBO) process (to be explained later in Section 2.2). Two other laminate samples were manufactured from the 1 wt% CNF Z-threaded CFRP (i.e., ZT-CFRP) prepregs, and one of the two ZT-CFRP prepreg sets (two 10-inch x 20-inch prepregs as a set) was exposed to RH identical to the traditional CFRP prepreg's RH exposure before the OOA-VBO curing. The find sample manufacturing

process was identical to the previous method (ZT-CFRP sample). However, only 16 layers of prepreg (10-inch x 20-inch prepregs as a set) were used to manufacture the final laminate. Unidirectional HexTow^{TM} AS4 Carbon fabric (1.79g/cm^3 fiber density, 3k Tow-size, and 190 g/m^2 areal weight) was used for all five samples. The matrix consisted of EPON 862 epoxy and Epikure-W curing agent, which were both purchased from Miller-Stephenson Chemical Co. The CNF PR-25-LD-HHT, purchased from Pyrography Products/Applied Sciences, Inc., has an average diameter of 100 nm and average length ranging from 50um to 100um. Disperbyk-191, and Disperbyk-192 (provided by BYK) was used for enhancing the CNF dispersion in the resin. According to [14], the CNF was reported to have a tensile strength of 2.35 ± 0.4 GPa, and a Young's modulus of 245 ± 52 GPa.

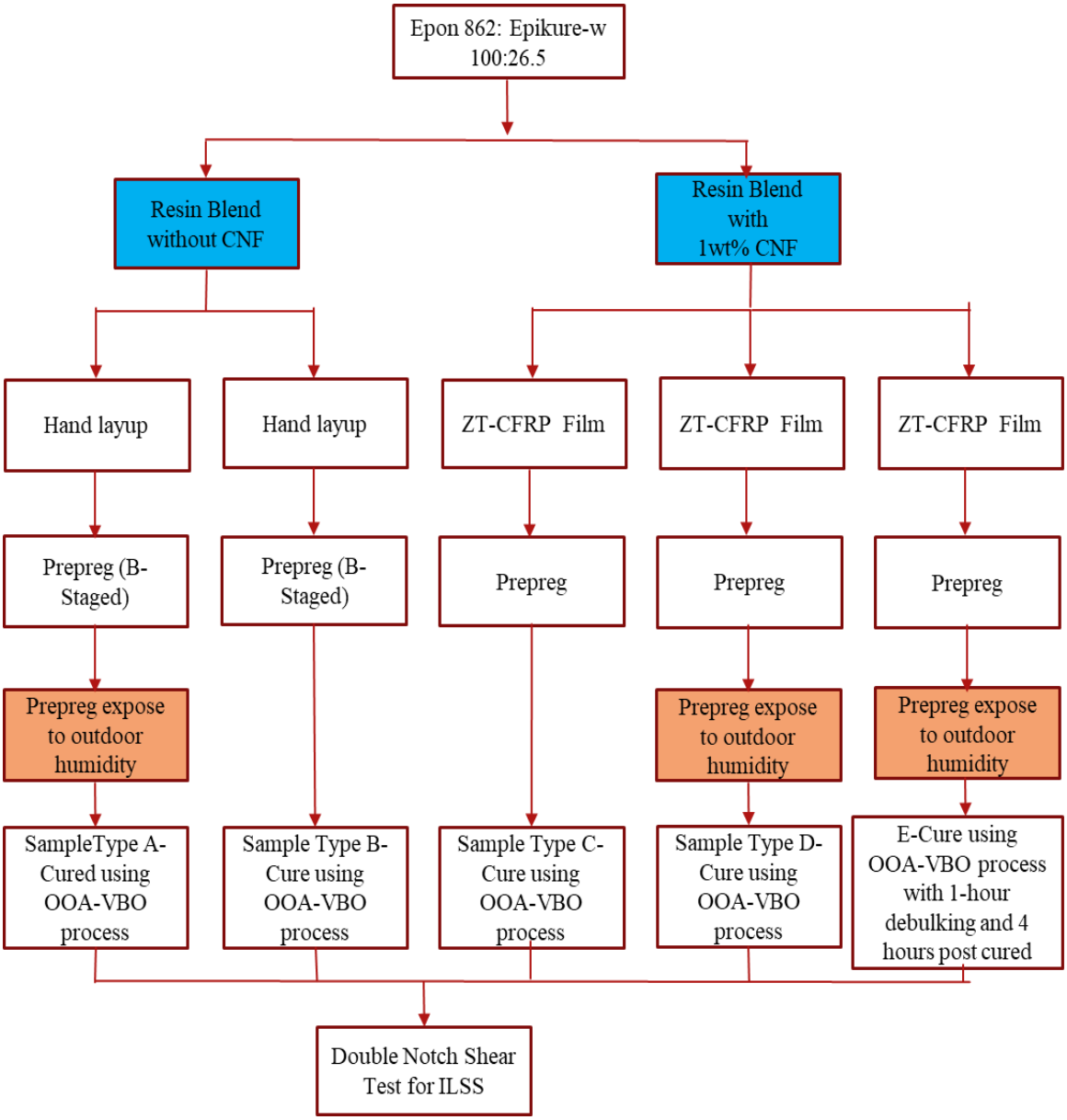

Figure 2. The entire process of manufacturing traditional CFRP and ZT-CFRP laminates for double notch shear test.

2.2 Methods

2.2.1 CFRP Manufacturing

The manufacturing of all five samples was divided into the traditional CFRP prepreg manufacturing and the ZT-CFRP prepreg manufacturing. The control CFRP prepreg (i.e., traditional CFRP prepreg) manufacturing process was done in several stages. First, mechanically mixed Epon 862 and Epikure-W according to the weight ratio of 100:26.5 for 10 minutes. In the following stage, the mixed resin blend was poured in a proprietary moisture removal apparatus placed into the vacuum chamber at 110-degree Celsius to remove unwanted bubbles introduced by mechanical mixing. In this final stage, four individuals 10-inch x 20-inch previously specified unidirectional carbon fiber fabrics were carefully impregnated with resin using a resin roller to ensure that carbon fiber fabric is wetted completely. Afterward, the impregnated prepregs were placed on a preheated (120 degree Celsius) hot plate for 40 minutes to get B-staged. Among all four B-stage prepregs, two of them were brought to outdoor exposure with RH-71.37% for 24 hours and the other two left in the laboratory room for 24 hours in a sealed condition. The two exposed prepreg samples were cut into 20 pieces, stacked, and cured using the OOA-VBO process. The exact same technique was used for the two CFRP prepregs stored and sealed in the lab and their CFRP laminates.

The patented [15] ZT-CFRP prepreg manufacturing process [6] is different from the control prepreg manufacturing process for z-threading the CNFs into the CFRP prepreg. An overview of ZT-CFRP manufacturing is illustrated in Figure 3. The prepreg

manufacturing process starts with mixing of Epon 862 with surfactants (BYK-191 and BYK-192) and the CNFs using a stirrer before being placed into an electrically operated high shear mixer. The surfactants BYK-191, BYK-192 to CNFs weight ratio of 1:1:1 has been proven to be an ideal ratio to get a homogeneous resin blend that can help to avoid entanglement of CNFs during the dispersion process. Next, the resin mixture was blended with a high shear mixture for an hour, 30 minutes clockwise and 30 minutes counterclockwise. In the following stage, the mixture went through a sonication process for an hour in an ASONICA Q700 Sonicator to break aggregations. Afterward, the Epikure-w curing agent (26.5:100 against the Epon 862 weight) was added to the sonicated resin mixture and blended with a high shear mixer for 10 minutes to get a homogeneous mixture. The mixture was degassed in a vacuum oven assisted by the proprietary moisture removal apparatus for 10-15 minutes to remove any air bubbles introduced by the previous process. Following that, the CNF-resin mixture was placed in a vacuum oven at 120 degrees Celsius temperature for approximately 45 minutes to get B-staged. This B-stage resin mixture has been used to manufacture CNF-resin films. In the following steps, the randomly aligned CNFs resin film was passed through a strong electrical field to align the CNFs in the Z-direction (through thickness direction) to form the ZT-resin film [6]. This process was done in a proprietary R2R automated assembly line developed by Hsiao group. These ZT-resin films were used to impregnate eight pieces of 10-inch x 20-inch unidirectional carbon fiber fabric using a one-directional non-isothermal flow transfer technique described in [6]. From this, eight prepreg samples were produced, six of them were exposed to outdoor RH for approximately 24 hours and other two prepregs were stored in the laboratory in a sealed condition. The following day, the exposed prepreg

samples and the laboratory prepregs were cut and cured into three different ZT-CFRP laminates (exposed and unexposed) using the OOA-VBO process.

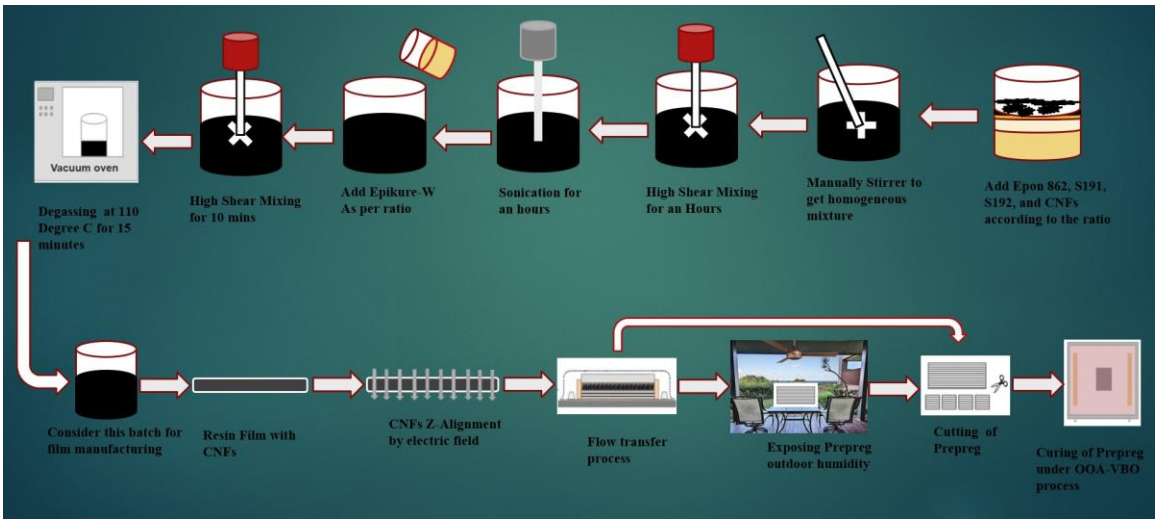

Figure 3. The flowchart of the ZT-CFRP prepreg and laminate manufacturing process.

Figure 4(a) shows the six small pieces trimmed from the ZT-CFRP prepregs for the CNF alignment observation/quality control. Figure 4(b) shows the microscopy side-view of the ZT-CFRP prepreg. One can observe many CNFs -threading through the carbon fibers along the z-direction.

(a)  (b) 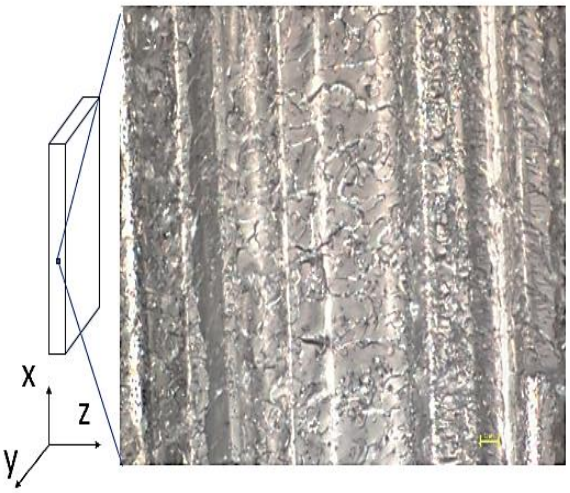

Figure 4. (a) Four small pieces of ZT-CFRP prepreg samples trimmed from the five larger 10” by 20” ZT-CFRP prepregs for alignment observation/quality control. (b) The side-view microscope picture of a small ZT-CFRP prepreg shows many CNFs z-threading through the carbon fibers in the z-direction.

The OOA-VBO setup is shown in Figure 5. The peel ply was used for easily separating the cured laminate from the distribution media layer and the vacuum bag. The curing cycle for four laminates curing was done in the same three stages. First, the assembly was under full vacuum at room temperature (around 23 degrees Celsius) for 10 minutes for debulking and removing the excessive air trapped when stacking the prepreg plies; but the 10-minute duration was kept relatively short compared with a typical hour-long debulking/degassing in OOA-VBA since the experiments require the moisture to be presented during the OOA-VBO curing to compare the effect of moisture. In the second step, the assembly was placed between two preheated (120 degree Celsius) hot plates of a

hot press (to simulate the oven effect) for 2 hours curing under full vacuum. In the third step, the composite laminate was post-cured at 180 degree C without vacuum for two hours, which was also shorter than the commonly used four hours of post-curing so the final curing could show some difference due to moisture. The last ZT-CFRP exposed prepreg went through an identical process. However, it went through an hour debulking phase and four-hour post cure.

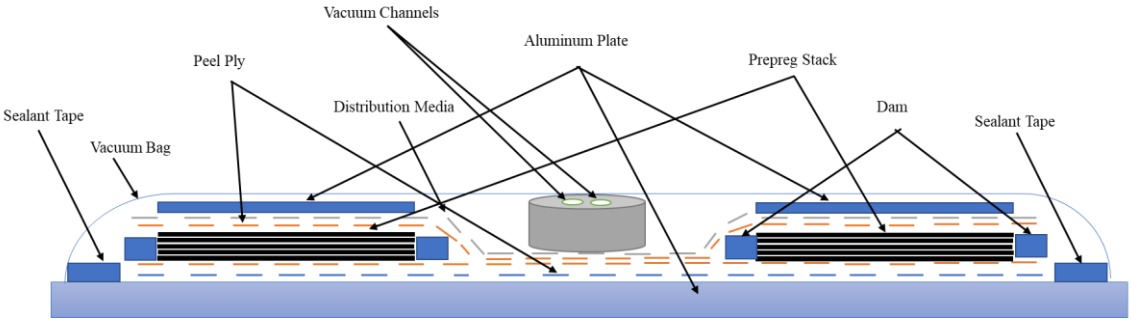

Figure 5. Schematic of OOA-VBO Setup used to cure all samples

Table1. Cure cycle overview of the OOA-VBO process used for five Laminates.

2 CFRP and 2 ZT-CFRP laminates			1 ZT-CFRP laminates 1-hour Debulking and 4-hours post-cured		
Time (minute)	Temperature (OC)	Vacuum (Bar)	Time (minute)	Temperature (OC)	Vacuum (Bar)
10	23 (Room Temp.)	1	60	23 (Room Temp.)	1
120	120	1	120	120	1
120	180	0	240	180	0

2.2.2 Preparation of Double Notch Shear (DNS) Test Samples

Once the laminates were cured, they were trimmed into small DNS test coupons and sanded down to the dimensions stated in the ASTM standard D-3846 [16] at 79.5 mm x 12.7mm. The standard had some leeway on the thickness at a range of 2.54 mm to 6.60 mm. Because of this, it was decided to sand down to the thickness of the thinnest sample to maintain consistency. The thickness chosen was 3.75 mm. After sanding the samples, the two notches were cut into place at approximately 6.30 mm away (the precise distance was measured on the shear fracture surface) and 1.1 mm in channel width. The thickness of final samples ranged from 3.74 – 3.87 mm with an average of 3.792 mm. The distance between the two notches was measured from 6.09 – 7.53 mm with an average of 6.64 mm. The notch cut measured from 1.32 – 1.78 mm with an average of 1.482 mm. The width measured 12.55 – 12.79 mm with an average of 12.696 mm. Due to the nature of the test, the cuts needed to have been uniform and at ideally a perpendicular arrangement with the surface. Otherwise, the samples could possibly produce invalid data as the unevenness could cause an inconsistent stress concentration effect at the edge of the shearing section (between the two notches). Additionally, it was important for the samples to maintain uniform thickness all over. If the thickness was not homogeneous, it would have offset the testing vice and led to poor results as the DNS sample could have shifted due to the imbalance and non-uniformness of holding.

CHAPTER III
EXPERIMENTATION AND ANALYSIS

3.1 Fiber Volume Fraction (FVF)

The fiber volume fraction (V_f) is the ratio of fiber in manufactured CFRP/ZT-CFRP laminate. In this report, the ASTM D792 has been used to determine the final laminate's fiber volume fraction, which is based on the Archimedean bouncy method [17].

To prevent fiber expansion, the OOA-VBO process was guided using dams and coal plate techniques in the laminate manufacturing process (Figure 5) for CFRP and ZT-CFRP laminate manufacturing. The fiber fabric expansion ratio r_e was unity 1 as there was no fiber fabric expansion in the final laminates. The fiber volume fraction (V_f) was calculated using Equation (2) based on AS4 fabric areal weight (A_w) 190 g/m^{2,} density of the fiber (ρ_f) 1.79 g/cm3, the number of plies (n) used, and the thickness (t) of the final laminates after cure.

$$r_e = \frac{Aw,manufacture}{Aw,actual} \quad (1)$$

$$A_{w,actual} = \frac{t * \rho_f * v_f}{n} \quad (2)$$

Table 2. Fiber Volume Fraction (V_f) for all five types of CFRP and ZT-CFRP sample.

Laminate types	Laminate thickness (t) cm	AS4 Areal Weight (A_w) g/cm2	Number of Ply used (n)	Fiber Density (ρ_f) g/cm3	Fiber Volume Fraction (V_f)
Control	0.4470	0.0190	20	1.790	47.49%
Control Exposed	0.4400	0.0190	20	1.790	48.25%
ZT-CFRP	0.4480	0.0190	20	1.790	47.39%
ZT-CFRP Exposed	0.3950	0.0190	20	1.790	53.74%
ZT-CFRP Exposed: and 1-hour debulked and post cured for 4-hours	0.3450	0.0190	16	1.790	49.23%

3.2 Shear Strength Testing

Shear strength testing can be conducted in many ways; some tests are more conclusive than others. This applies to the previously tested short beam shear (SBS) test at ref [6] and the double notch shear (DNS) test to be used in this study. The test is somewhat convoluted in its description where it is technically closer to an interlaminar shear strength (ILSS) test rather than, as the name implies, an in-plane shear strength test. This discrepancy stems from the position of failure for the sample, the region between the notches. This test is more complicated than the SBS test as the sample is intentionally given damage along its thickness. Too much damage would cause a stress concentration on the short end and could fail unevenly. This is to reduce the amount of compression force needed to split and break the sample. However, referring to the previous SBS tests, it seemed that some of the CFRP composite's carbon fiber buckled and pushed the delamination of the laminate on the compression side before the sample was destroyed by shear damage and that could affect the effectiveness of the short beam elastic model and

the SBS shear stress prediction. The DNS test is more strongly based on shear damage so it could avoid the disturbance on the shear strength identification due to other failure modes.

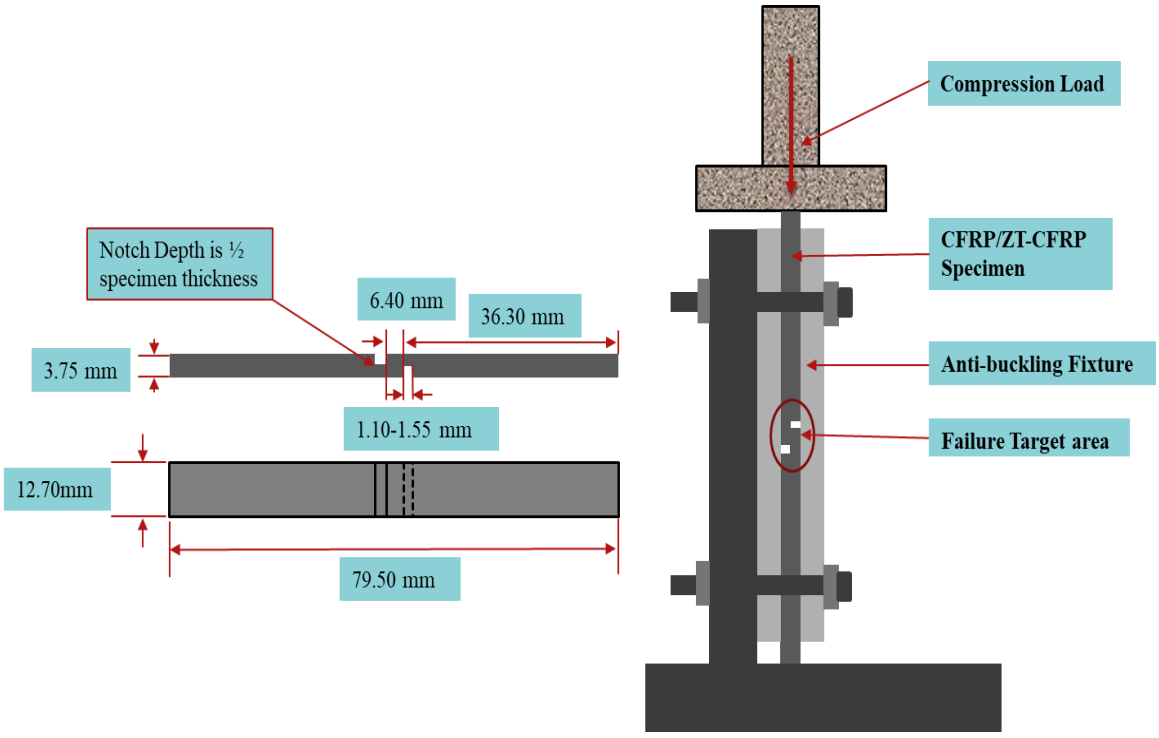

Figure 6. Double Notch Shear Testing apparatus defined by ASTM D3846 [16]

The testing apparatus for this new batch of testing is the TINIUS OLSEN Super "L" universal testing machine. This machine has a 5337N loading cell and runs the test at 13 mm/min following the standard. For each case there are five testing samples for satisfied sampling. Before testing, the samples were inserted into a modified ASTM D695[18] anti-buckling fixture.

The interlaminar shear strength (ILSS) was determined using the required compression force (F) applied to break the specimen divided by the area (A) between the notches.

$$ILSS = \frac{F}{A} \qquad (3)$$

3.2.1 Microscopic Morphology Study and Hardness Test

The failure mode of the sample owing to the DNS test was characterized and compared using a Nikon Eclipse LV150 optical microscope equipped with an extended depth of focus module.

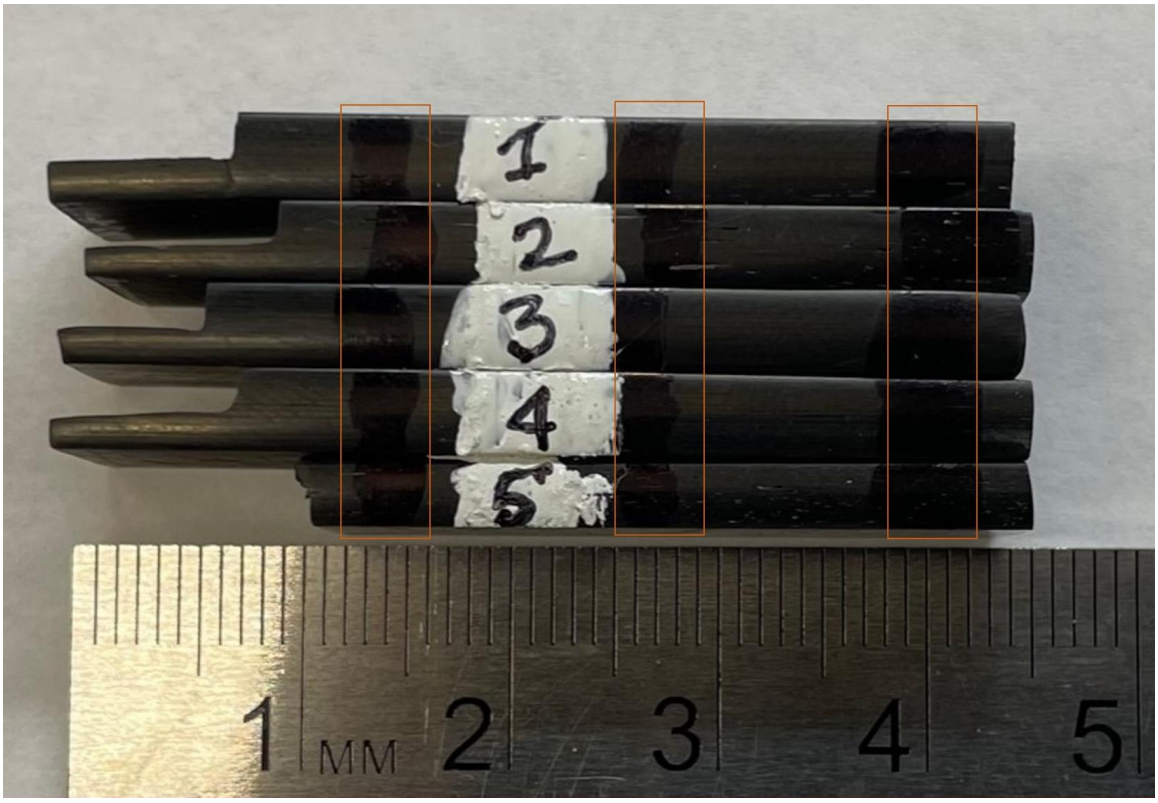

Figure 7: All five samples marked in three spots used for microscopic void analysis. 1) control sample, 2) Control prepreg RH exposed Sample, 3) ZT-CFRP Sample, 4) ZT-CFRP prepreg RH exposed sample, 5) ZT-CFRP prepreg RH exposed sample with 1-hour debulking and 4-hours post cured.

The microscopic analysis was completed in several stages. First the samples in the figure 7 were polished with 3M sandpaper starting with 220 grit followed by 800, 1500, 2000, and finally with 3000 grit. Sanding of all samples was done with similar hand pressure for one minute with each grade of sandpaper. Following that, all the samples were washed using detergent to remove the dust and particles. Then the samples were placed into a 100^{o}C preheated oven for approximately 30 minutes to dry completely. In the next steps the samples were marked (shown in Figure 7) using permanent markers to make the void area more noticeable and easily identifiable. Three spots were chosen on the pre-marked to provide a fair void fraction calculation from those spots. In the picture, the void area was chosen using an automated void identifying option in the microscope which marked the void in the picture with red marks.

Table 3: Void fraction of all five samples tested. The void content ranking is control (1.45%) < ZT-CFRP (2.12%) < ZT-CFRP Prepreg RH exposed (5.84%) < Control prepreg RH exposed (8.78%) < ZT-CFRP prepreg RH exposed 1-hour debulking and 4 hours post cured (10.05%).

	Control			Control Prepreg Exposed			ZT-CFRP			ZT-CFRP Prepreg Exposed			ZT-CFRP Prepreg Exposed, 1-hour debulked and 4-hours post-cured		
Calculated void Area μm^2	21973	25598	1845	147240	71938	80860	28468	7097	36798	142452	21083	36547	204437	43602	97235
Total Area μm^2	1133374	1143252	1135613	1139115	1137833	1141985	1140386	1136559	1137204	1140716	1144538	1143903	1147098	1144538	1142300
Void Fraction	1.94%	2.24%	0.16%	12.93%	6.32%	7.08%	2.50%	0.62%	3.24%	12.49%	1.84%	3.19%	17.82%	3.81%	8.51%
Mean Void Fraction	1.45%			8.78%			2.12%			5.84%			10.05%		

All five samples were analyzed for void fraction where each sample was examined in three different spots to get a fair non-biased void percentage calculation. The control tested sample had an average of 1.45% void (Table 3) which is close to the ZT-CFRP average void of 2.12%, which was a likely outcome as that prepreg was processed in room low RH conditions in the OOA-VBO process. The samples with prepreg outdoor RH exposed (control RH exposed-8.78%, ZT-CFRP exposed-5.84%, and ZT-CFRP RH exposed with 1-hour debulking and 4 hours post-cured-10.05 %) show a higher average percentage as those sample's prepreg absorbed moisture during the exposure outdoors.

.

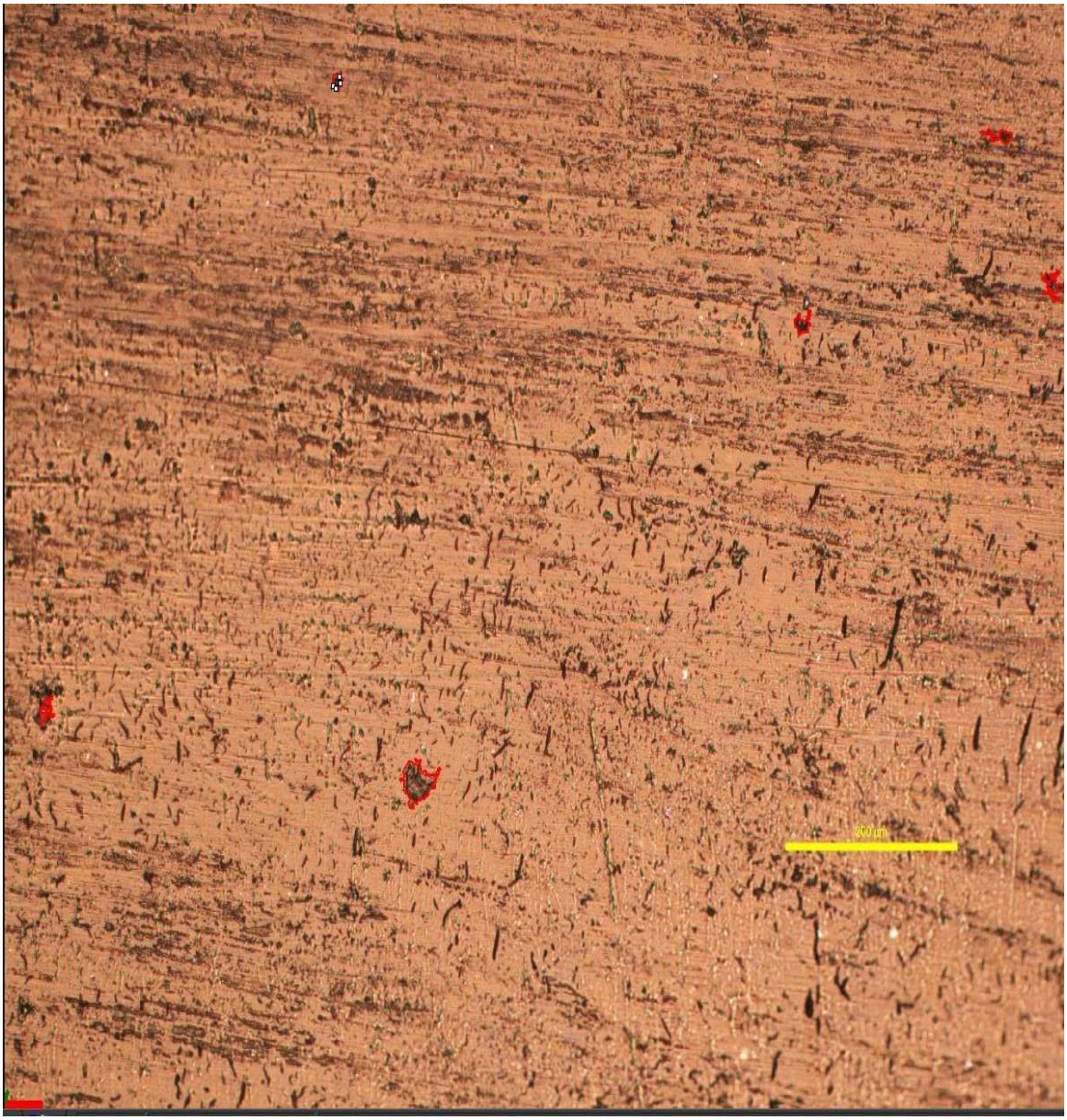

Figure 8. Image of hand-polished control prepreg specimen with voids taken at 100x magnification in the pre marked spots.

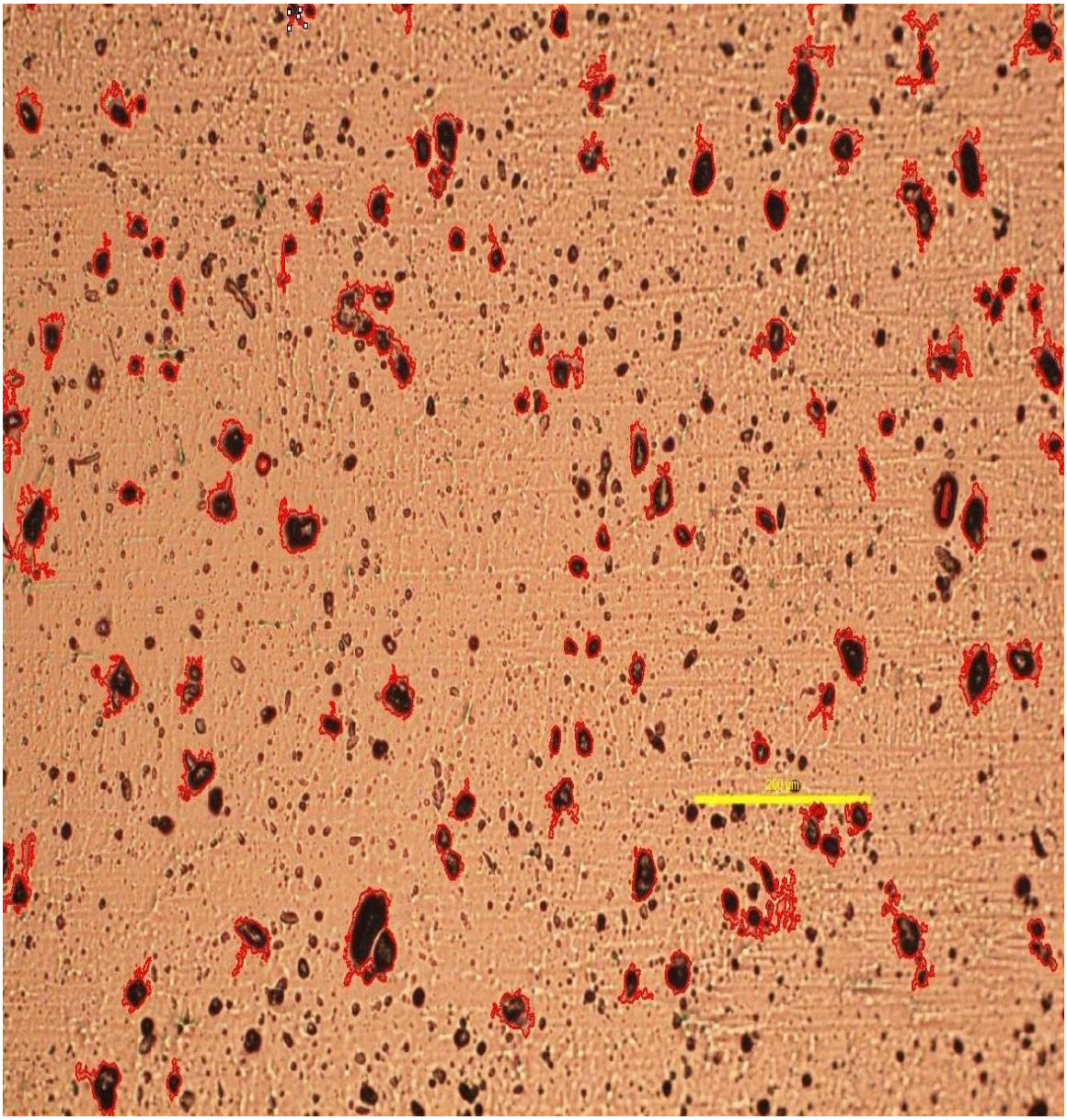

Figure 9. Image of hand-polished control prepreg RH exposed specimen with voids taken at 100x magnification in the pre marked spots.

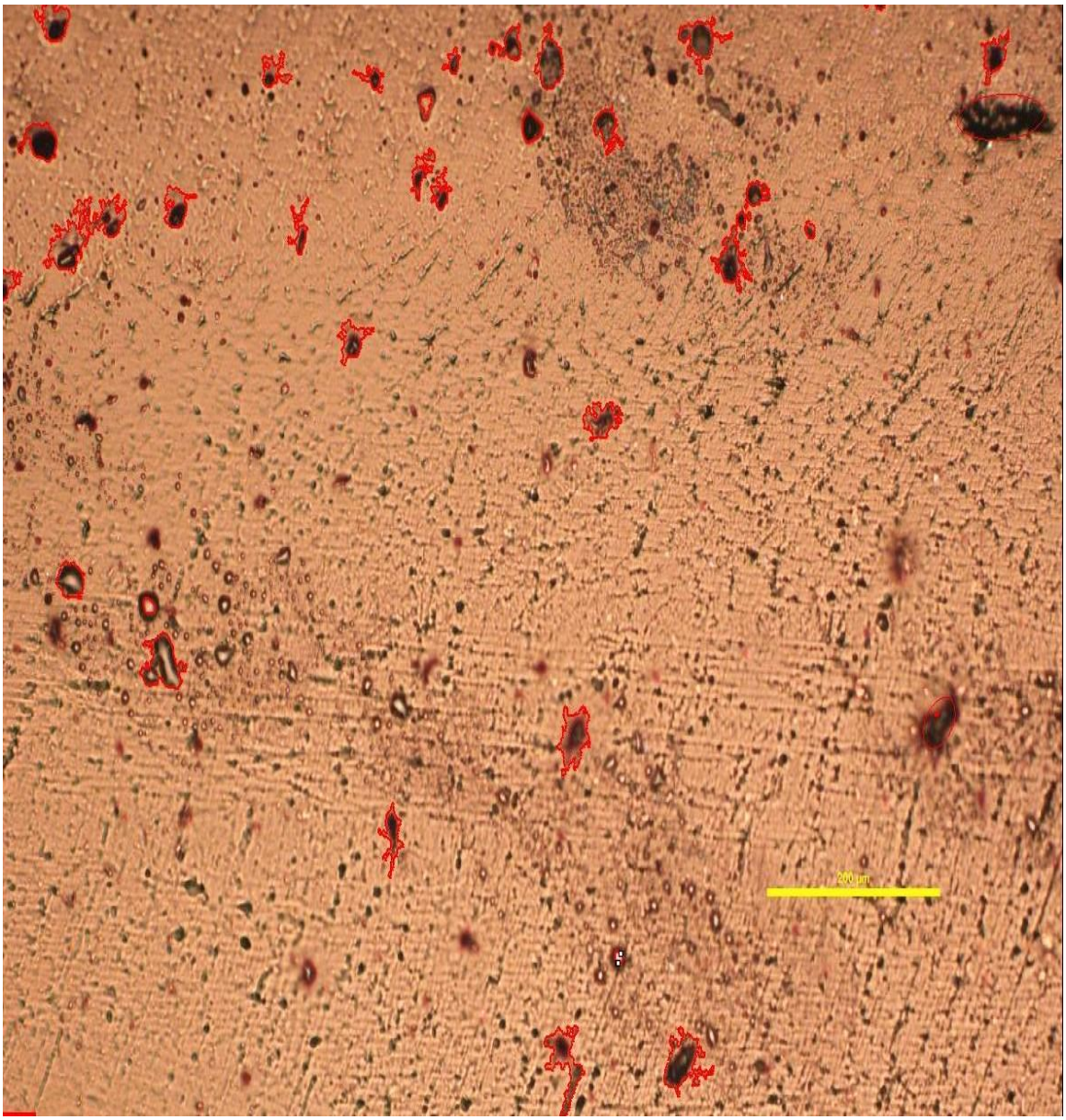

Figure 10. Image of hand-polished ZT-CFRP specimen with voids taken at 100x magnification in the pre marked spots.

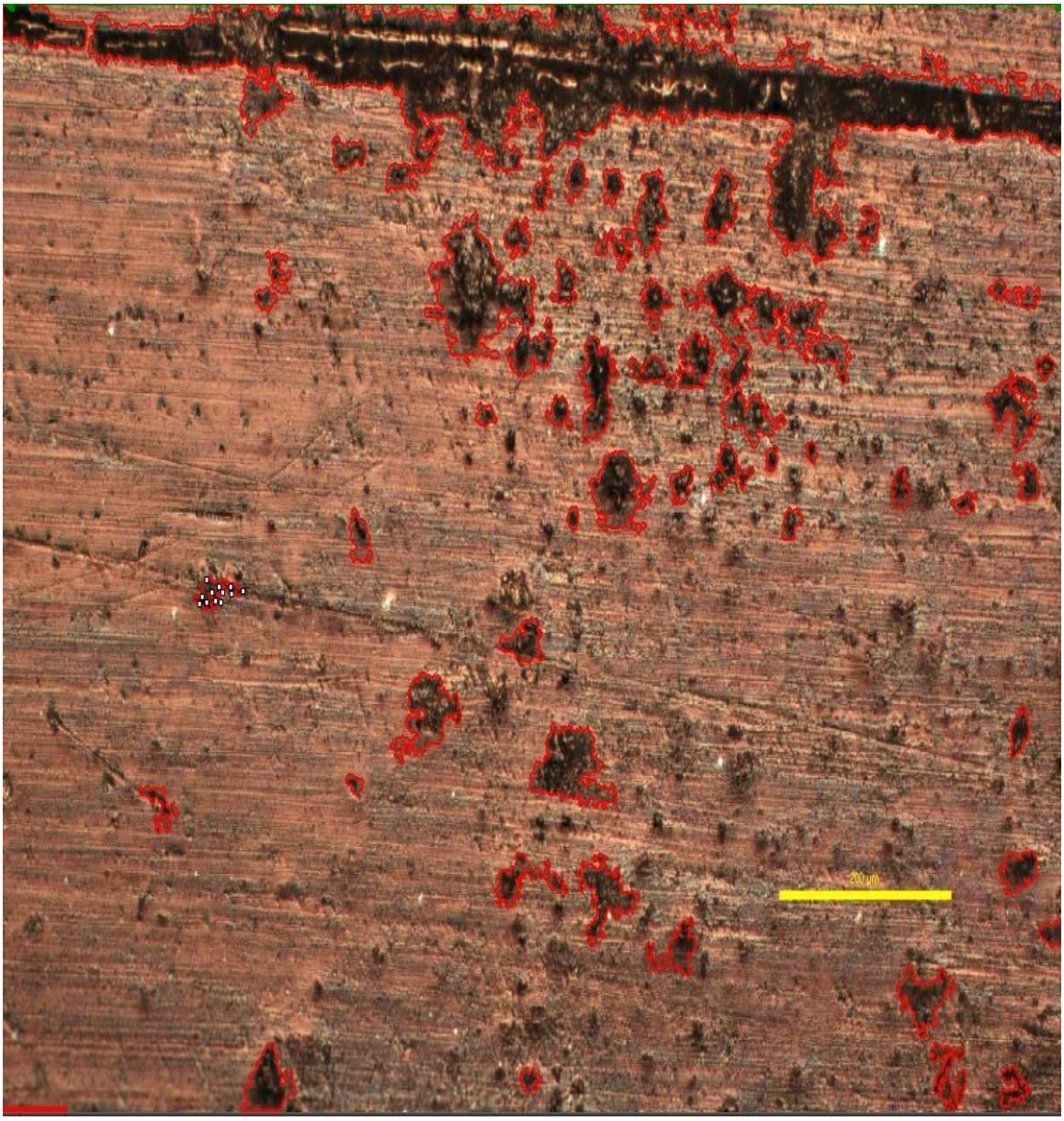

Figure 11. Image of hand-polished ZT-CFRP prepreg RH exposed specimen with voids taken at 100x magnification in the pre marked spots.

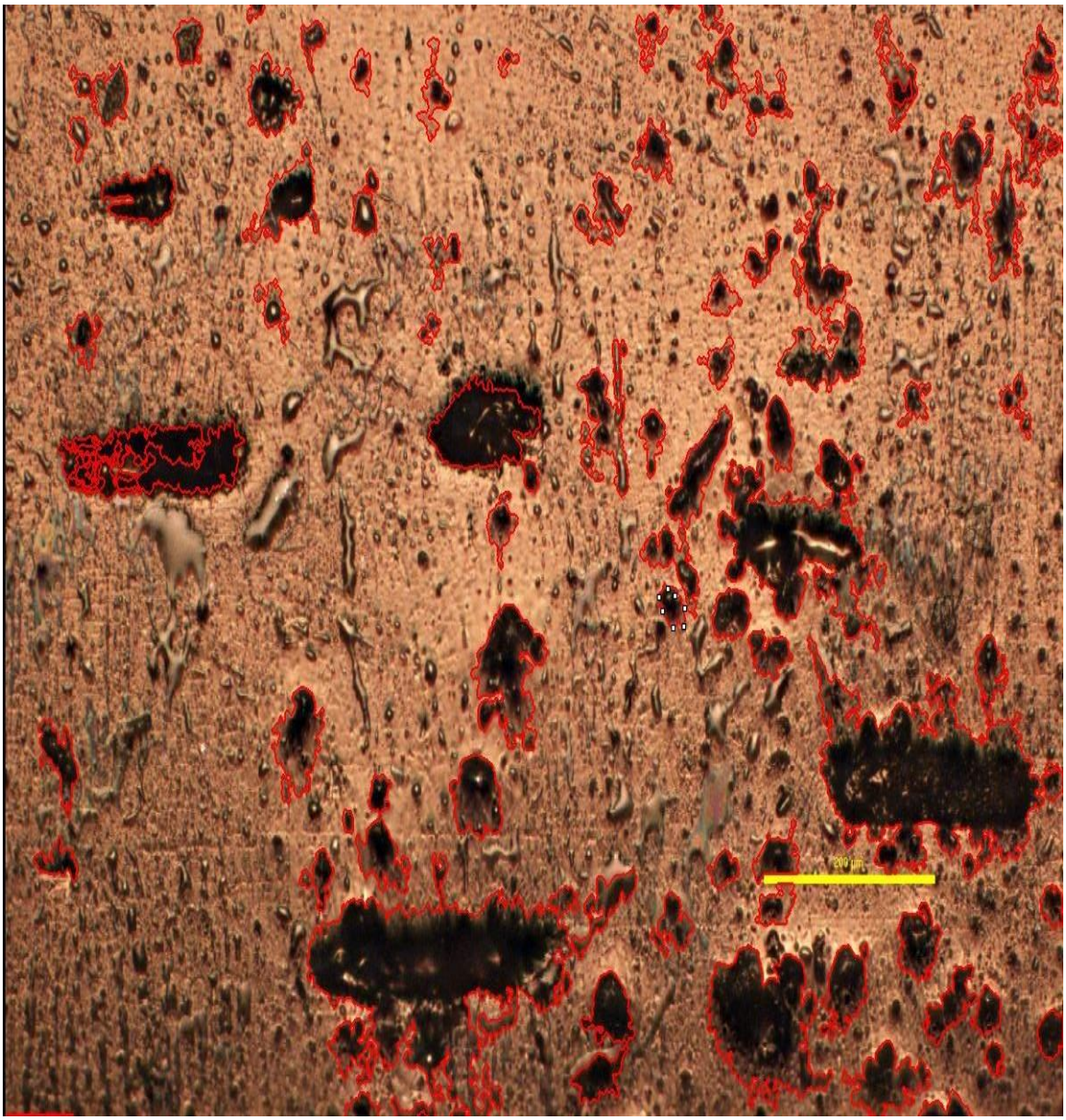

Figure 12. Image of hand-polished ZT-CFRP prepreg RH exposed 1 hours debulking and 4 hours post cured specimen with voids taken at 100x magnification in the pre marked spots.

The laminate DNS samples, after being fractured, were tested for their hardness (Table 4) using the digital durometer hardness tester (Model DD-D-A-W).

Table 4. The hardness data for all DNS tested samples. The mean hardness ranking shows that Control CFRP exposed (99.82) > ZT-CFRP prepreg exposed (99.74) > Control CFRP (99.7) > ZT-CFRP exposed and hour debulked (99.56) > ZT-CFRP (99.38).

	Control CFRP Hardness %	Control CFRP Prepreg Exposed Hardness %	ZT-CFRP Hardness %	ZT- CFRP Prepreg Exposed Hardness %	ZT- CFRP Prepreg Exposed, an hour debulked, 4 hours post cured Hardness %
Sample- 1	99.7	99.9	99.6	99.8	99.6
Sample-2	99.5	99.8	99.6	99.7	99.3
Sample-3	99.7	99.8	98.6	99.7	99.6
Sample-4	99.8	99.7	99.8	99.7	99.6
Sample-5	99.7	99.9	99.3	99.8	99.7
Mean	99.68	99.82	99.38	99.74	99.56
STD V	0.110	0.084	0.471	0.055	0.152
CoV	0.110%	0.084%	0.474%	0.055%	0.152%

CHAPTER IV

RESULTS

The carbon fiber volume fraction of five types of samples were calculated (see Table 2) as control CFRP 47.49%, control CFRP prepreg RH exposed 48.25 %, ZT-CFRP 47.39%, ZT-CFRP prepreg RH exposed 53.74%, and ZT-CFRP prepreg RH exposed with long debulking and then post cured 49.23%. The considerations for these samples are, but not limited to, the fabric areal weight, total number of plies, and the laminate thickness, assuming there was no fiber expansion since the OOA-VBO process was guided by dams and caul plate. Table 5 shows the ILSS test data of all types of samples with five specimens each. Table 6 removes the maximum and minimum ILSS values samples from the list shown in Table 5 to omit any potential outliers. This would provide a fair representative comparison for all samples. The hardness values of the CFRP samples were added into Table 6. These outliers could be due to improper fitting of the testing fixture and the sample, cutting of the notches, or an unexpected scenario involved in the testing/facture process. The ILSS results of Table 5 are graphically presented in Figure 12. From Table 5 and Figure 12, one can see that the control CFRP samples without prepreg RH exposure had the average ILSS of 67.08 MPa with coefficient of variance (C.O.V.) of 1.79%, which displayed a very repeatable set of ILSS measurements. For the samples of the control CFRP with the prepreg RH exposure, the ILSS increased to 74.06 MPa (a 10.40% increase), but the C.O.V. increased to 4.11%. As shown in the literature [3], a small amount of moisture can enhance the resin curing process and increase the ILSS. This increase of ILSS statistical

mean was reasonable and the uncertainty of moisture introduction caused an increase in C.O.V. The samples of ZT-CFRP without prepreg RH exposure increased the ILSS statistical mean by 10.40%, but further increased the C.O.V. to 6.04%. It should be noted that, these sets of CFRP had a potentially shorter post-curing (180^{o}C by two hours, rather than the more commonly used four hours 180^{o}C post-cure) and the added surfactants could slow the curing process. This could be supported by the lowest hardness values of the ZT-CFRP samples (see Table 4). At this point it is hypothesized that with long debulking and 4 hours 180 ^{o}C post-curing, it is possible the ILSS mean and C.O.V could be improved. The ZT-CFRP prepreg with RH exposed increased compared with the control laminate samples' ILSS statistical mean to 71.53 MPa (a 6.63% increase) and decreased (by 3.38%) compared to ZT-CFRP without prepreg RH exposed. This increase in ILSS was enhanced by the Z-threaded CNFs reinforcement. The decrease in ILSS was correlated with the increase of void fraction in ZT-CFRP prepreg RH exposed laminates. The hardness values increased for the ZT-CFRP prepreg RH exposed samples compared with ZT-CFRP samples. However, it is hypothesized the moisture would help the curing process and the CNF would help the ILSS. This could be disappointing as the ILSS of this set of ZT-CFRP prepreg with RH exposure did not produce the highest ILSS value among all four types of samples (control, control prepreg exposed, ZT-CFRP, ZT-CFRP prepreg exposed). However, as one reviewed the OOA-VBO process, it was noticed that the room temperature dwelling stage (debulk/de-gas) was merely 10 minutes, which was an inadequate time compared to the usual OOA-VBO practice of debulk/de-gas stage at longer intervals of time to potentially remove all moisture/voids within the laminate. Given that the CNF has a hollow tube structure, the excessive moisture could be trapped in the CNF

which would not be removed by the short debulk/degas process. The excessive moisture, as supported by the literature [4], can cause an adverse effect to the ILSS, possibly due to voids, and inhibit the maximum achievable degree of cure near the water pockets [2]. The assumption made previously of sufficient debulking/degassing and long post-cure may improve ZT-CFRP RH exposed prepreg ILSS. To identify the long debulking and post-cure effects, one set of ZT-CFRP RH exposed prepreg was manufactured and tested. However, the ILSS results dropped to 61.23 MPa (17.28% decreased compared to ZT-CFRP) with an C.O.V. of 2.88%. This drop of ILSS (Figure 12) is supported by the increase of void fraction in the microscopic picture and the hardness test results from Table 6.

Table 5. Original ILSS data for all types of samples, including potential outliers

Laminate Materials	Contol CFRP	Control CFRP prepreg Humidity Exposed	ZT-CFRP	ZT-CFRP Prepreg Humidity exposed	ZT-CFRP Prepreg Humidity exposed an hour Debulked 4 hours Post cure
sample 1	66.83635072	70.57690531	79.48048341	70.37459244	60.0089813
sample 2	71.86852208	71.50565068	73.99448766	79.32455451	63.25915755
sample 3	68.38188165	77.42943256	78.52052531	72.39341874	60.4474694
sample 4	61.11466503	73.23864951	54.36359225	70.82212494	64.09427007
sample 5	66.02379887	83.06718145	69.57344308	71.35962672	59.36367418
Mean	66.84504367	75.1635639	71.18650634	72.85486347	61.4347105
Standerd deviation	3.908611142	5.14111838	10.19895902	3.694229845	2.103473574
C.O.V.	5.85%	6.84%	14.33%	5.07%	3.42%
ILSS relative drop due to prepreg humidity exposure (%)		12.44%		2.34%	-13.70%
ILSS relative change from the Control CFRP without humidity exposure	N.A.	12.44%	6.49%	8.99%	-8.09%

Table 6. Original ILSS data for all types of samples (after removing the potential outliers, i.e., the maximum and the minimum ILSS values for each type of sample) and the hardness tested results for all 25 samples

Laminate Materials	Contol CFRP Shear Strength (MPa)	Control CFRP Hardness %	Control CFRP prepreg Humidity Exposed Shear Strength (MPa)	Control CFRP Prepreg Exposed Hardness %	ZT-CFRP Shear Strength (MPa)	ZT-CFRP Hardness %	ZT-CFRP Prepreg Humidity exposed Shear Strength (MPa)	ZT- CFRP Prepreg Exposed Hardness %	ZT-CFRP Prepreg Humidity exposed an hour Debulked 4 hours Post cure	ZT- CFRP Prepreg Exposed, an hour debulked, 4 hours post cured Hardness %
sample 1	66.84	99.70	*	99.90	*	99.60	*	99.80	60.0089813	99.6
sample 2	*	99.50	71.51	99.80	73.99	99.60	*	99.70	63.25915755	99.3
sample 3	68.38	99.70	77.43	99.80	78.52	98.60	72.39	99.70	60.4474694	99.6
sample 4	*	99.80	73.24	99.70	*	99.80	70.82	99.70	*	99.6
sample 5	66.02	99.70	*	99.90	69.57	99.30	71.36	99.80	*	99.7
Mean	67.08	99.68	74.06	99.82	74.03	99.38	71.53	99.74	61.23853608	99.56
Standerd deviation	1.20	0.11	3.05	0.08	4.47	0.47	0.80	0.05	1.763590455	0.152
C.O.V.	1.79%	0.11%	4.11%	0.08%	6.04%	0.47%	1.12%	0.05%	2.88%	0.15%
ILSS relative change due to prepreg humidity exposure (%)			10.40%				-3.38%		-17.28%	
ILSS relative change from the Control CFRP without humidity exposure	N.A.		10.40%		10.36%		6.63%		-8.71%	

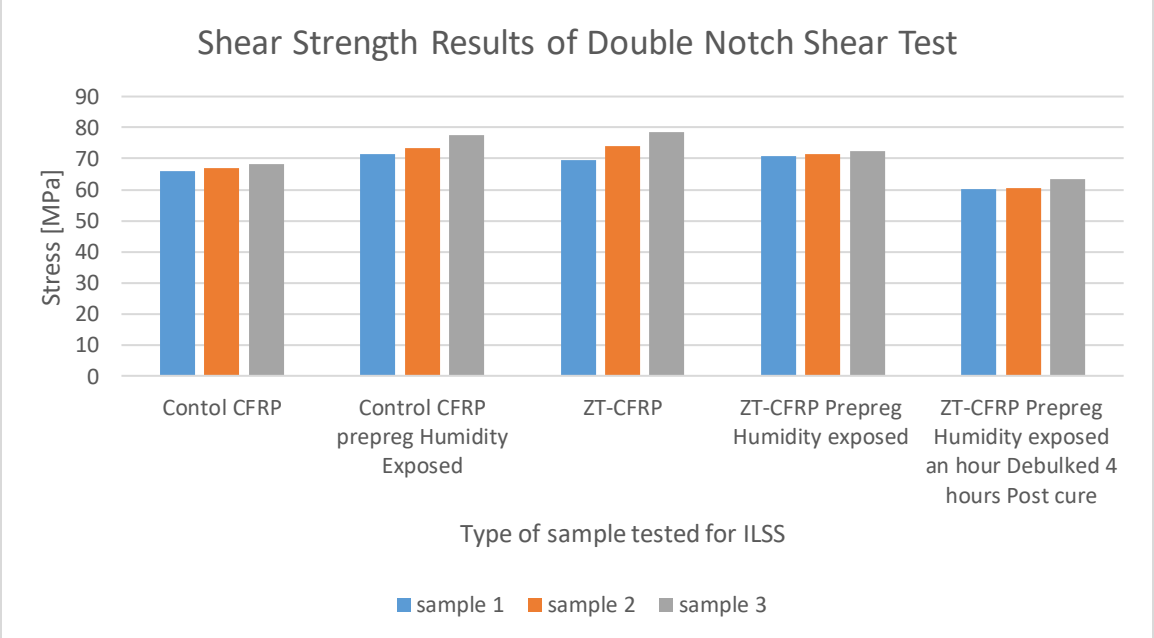

Figure 13. Double Notch Shear Test ILSS results comparison of selected three samples from each case after removing the potential outliers (i.e., the maximum and minimum).

Figure 14 shows the shear stress Vs crosshead displacement curves for all types of samples, three samples for each case. The sample's shear fracture moment can be easily identified in the end peak by sudden drop of the shear stress. However, some samples experienced laminate buckling right at the notch sections, and some did not. Those experiencing the notch section laminate buckling were failed due to the high force moment of the imbalanced compressive stress acting on the notched laminate section. However, the bucking notch section can still provide the compressive/shear load on the sample until its shear-failure at the targeted area due to the guide of the testing fixture supporting its further buckling induced separation/breakage; Under such scenario, the overall compressive stiffness of the DNS sample is reduced due to the buckled notch laminate section, but the final shear strength seemed not to be affected if one compares the three curves of the control CFRP case. It is interesting that all CFRP with RH exposure did not have any single notch laminate bucking issue. This likely caused by the more complete cure of the resin matrix. On the other hand, since all the ZT-CFRP samples have the buckling issue, as also indicated previously, it is possible that the added surfactants may require the composite to be post-cured longer than two hours.

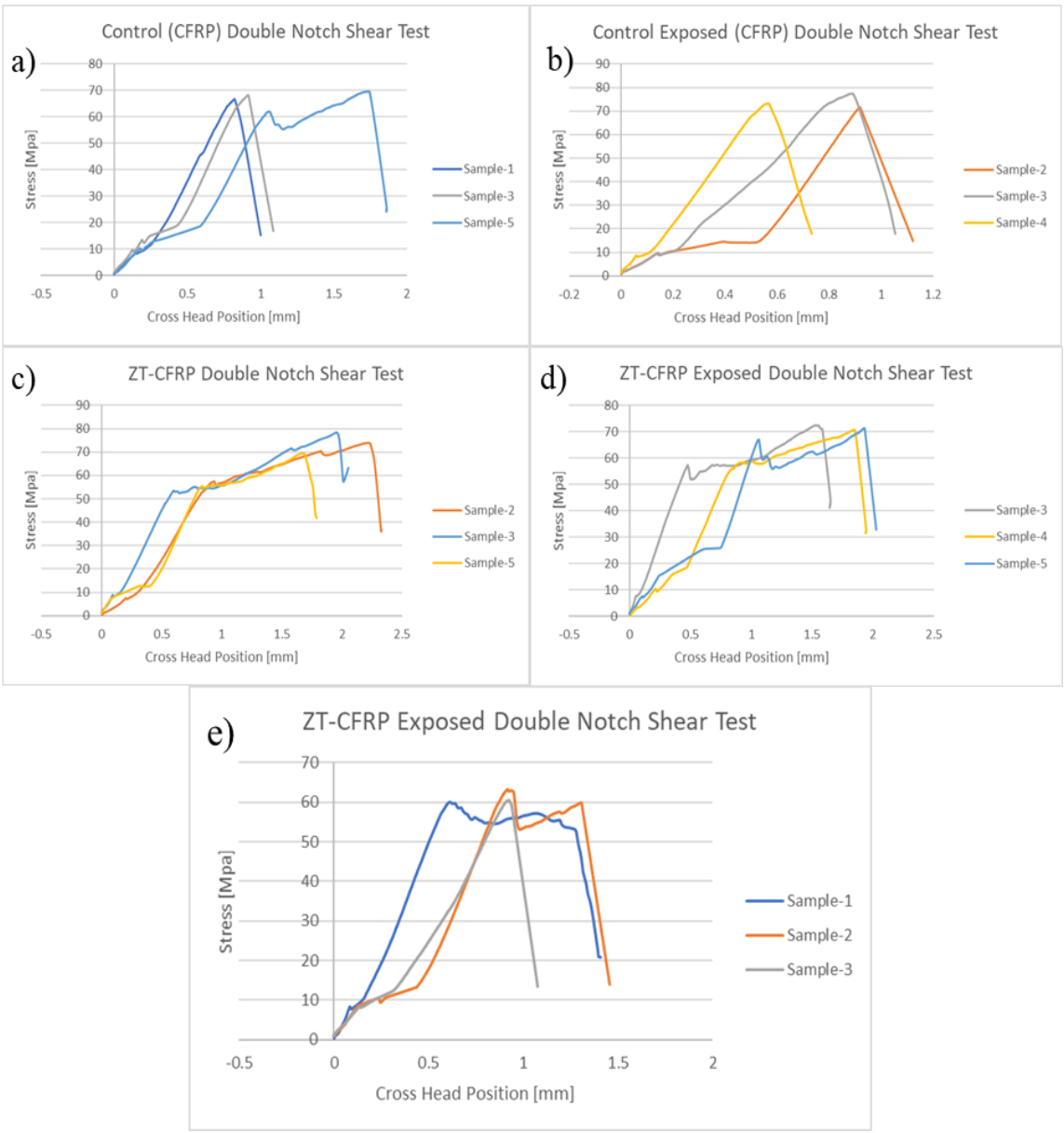

Figure 14. Shear stress Vs crosshead displacement during the DNS tests for a) control CFRP samples, b) control CFRP/prepreg-exposed samples, c) ZT-CFRP samples, d) ZT-CFRP/prepreg-exposed samples, e) ZT-CFRP/prepreg RH exposed samples which have been debulked for an hour and post-cured for four hours.

The fracture surfaces of the five types of laminate samples were examined by microscopy and are shown in Figure 15. Figure 15a shows the side-view of the control CFRP DNS sample, which has a clean and straight crack due to the shear. Figure 15b shows the top-view of a fractured DNS sample and reveals a void triggered by a complex fracture surface near it. Figure 15c shows the close-up top-view of a ZT-CFRP DNS fractured sample. It shows that the carbon fiber tow was broken and the snapped CNFs, which were previously embedded in the resin and carbon fiber bed, were pulled out from the other side of the broken/fractured carbon fiber tow. The majority of the CNF pullout lengths, under this fracture mode, were about 5-10 micrometers, which is close to the diameter of the AS-4 carbon fiber (7 micrometers). Figure 15d shows the side-view of the ZT-CFRP prepreg RH exposed DNS fracture sample. It shows that a fiber layer fractured and that the crack propagation was redirected due to the additional fracture resistance provided by the CNF z-threads. From the microscopy analysis one can see that the control CFRP has a clean and straight crack propagation, which may also explain its lowest shear strength measured in the double notch shear (DNS) tests.

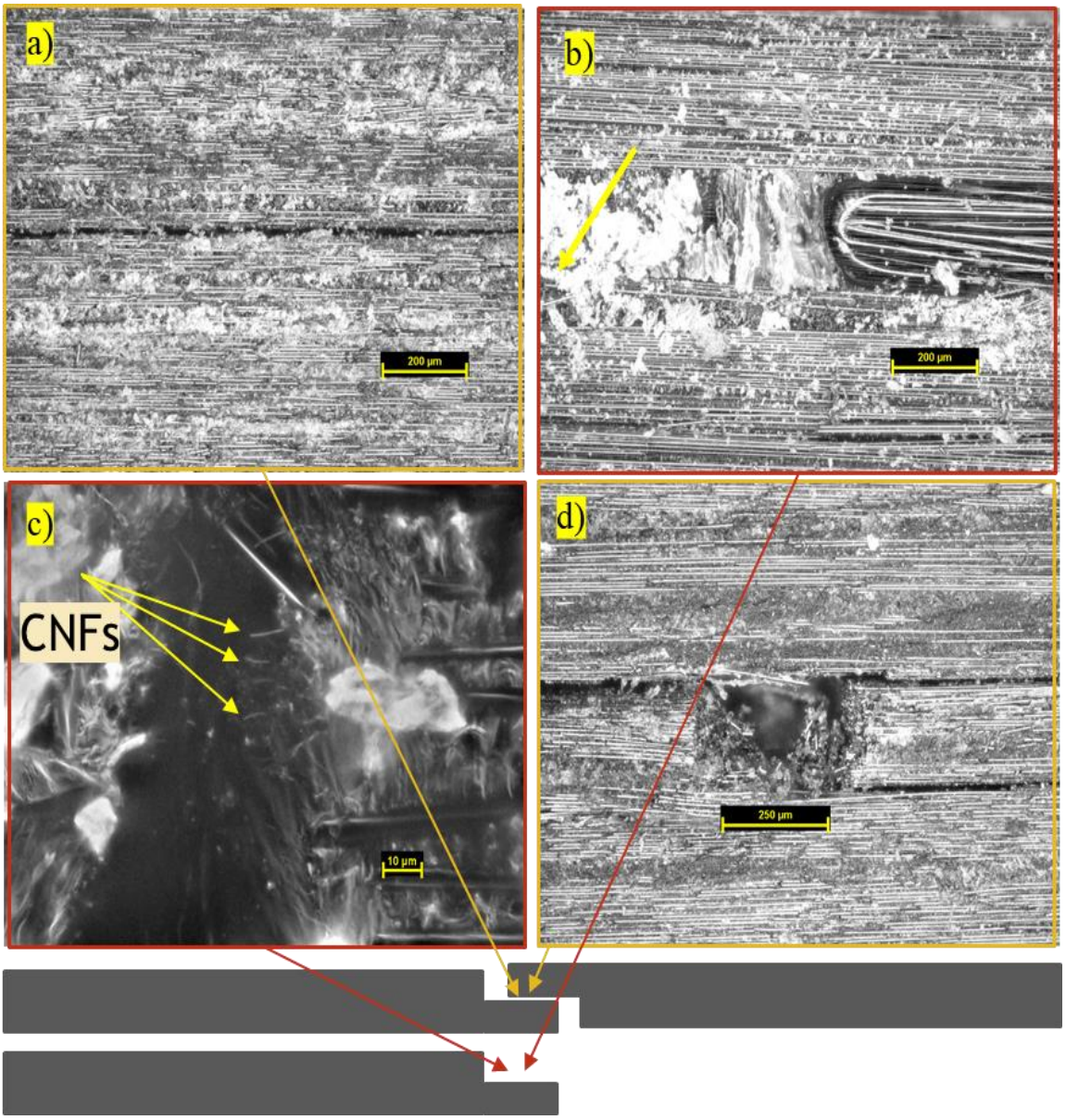

Figure 15. Microscope pictures of the fracture surfaces of the five types of DNS shear-tested composite laminate samples. a) The control CFRP sample has a clean shear crack. b) The control CFRP prepreg RH exposed sample has a void in the crack zone and a complex fracture surface nearby. c) The carbon fiber tow fractured in the crack zone and on the shear-fracture surface, whereas the CNFs were fractured and pulled out (pullout lengths were about 5-10 micrometers) from the other side of the resin matrix and carbon fiber bed. d) The ZT-CFRP prepreg RH exposed DNS sample showed a fiber layer fractured and the crack propagation was redirected due to the additional fracture resistance provided by the CNF Z-threads.

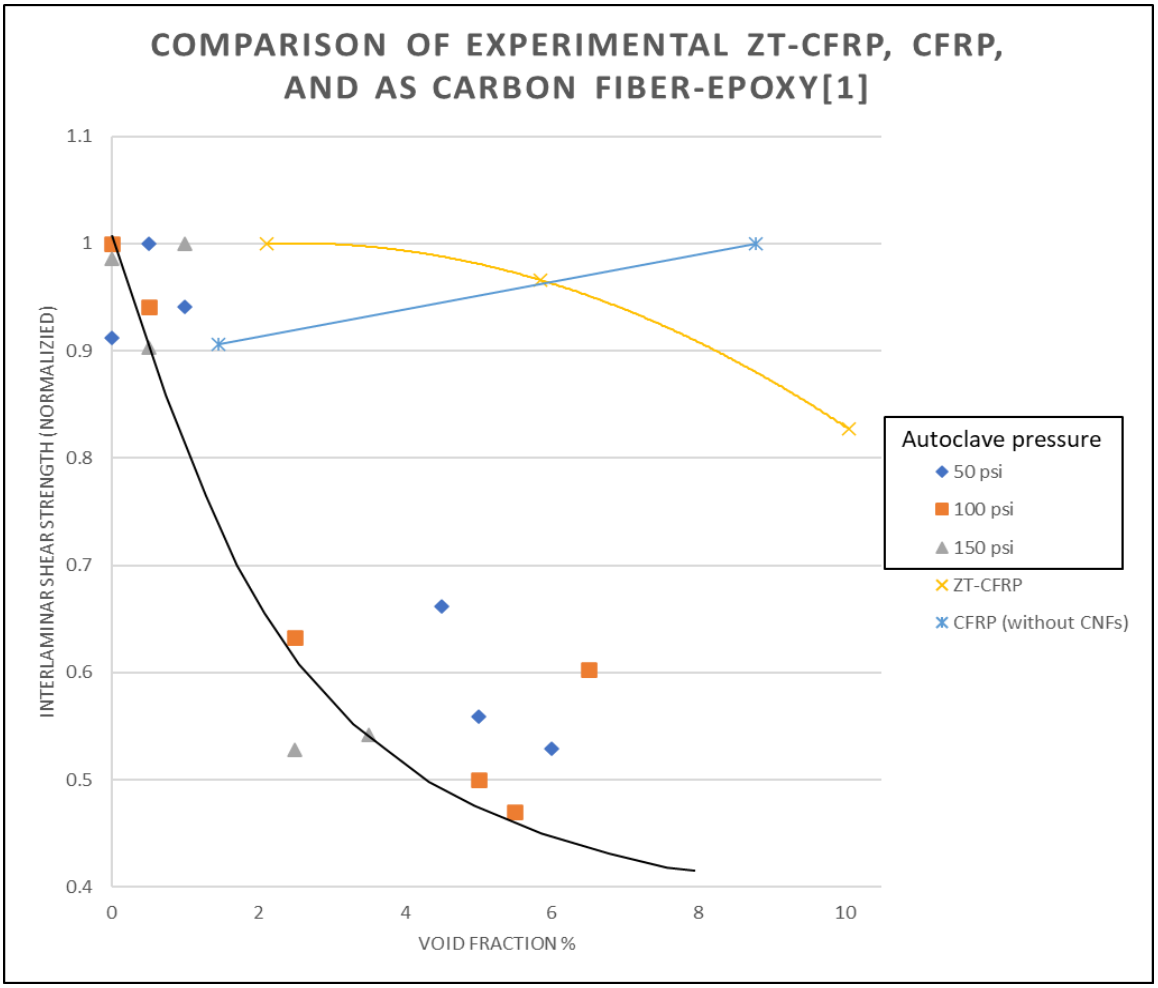

Figure 16: Literature reported traditional autoclaved CFRP laminates' ILSS relationship with void fraction due to autoclave pressure control "normalized curve" and the CFRP and ZT-CFRP laminates' normalized ILSS curve with different void fractions induced by moisture exposure. The literature graphs' void fraction and its ILSS data is based on different autoclave pressure. The traditional autoclaved CFRP laminates' ILSS decreased to 42% with the change of void content from 0 to 8%. The ZT-CFRP laminate's ILLS gradually dropped to 85% of its 2-10 % void content caused by moisture exposure. The presence of a similar amount of moisture-induced void content (8% in both cases, CFRP 1-8% and ZT-CFRP 2-10%) in traditional CFRP laminate and ZT-CFRP laminate responds differently under shear load. It should be note that the ZT-CFRP has additional surfactants, which reduced the curing of the resin. On the other hand, the moisture enhanced the curing of the resin.

The strength of ZT-CFRP laminates and traditional CFRP laminates are susceptible to moisture/void as shown in Figure 15 and ZT-CFRP tested laminates outperform the traditional CFRP laminates with similar amounts of void/moisture when void contents were less than 6%. By analyzing experimental results, it appears that ZT-CFRP ILSS gradually decrease from 74.06 MPa to 61.24 with the increase of void fraction from 2.12% to 10.05% (Figure 15) due to prepreg RH exposure. Moreover, the hardness value increased with the moisture-induced void fraction increased slightly, which is supported by the literature [3]. The hardness of the ZT-CFRP dropped marginally at a void fraction of 10.05% indicating that tested laminates had more moisture than the limit (which has been reported in [3]) in which the moisture-induced degree of cure enhancement of ZT-CFRP is no longer effective. Control prepreg RH exposed CFRP have shown higher ILSS value and slightly better hardness compared to Control CFRP laminates (Table 4 and Table 6). The literature ILSS vs void fraction data/curved based on different autoclave pressure and the experimental data/curves from this prepreg-RH-exposure experiment concluded that regardless of the source of moisture/void the CFRP/ZT-CFRP laminates are susceptible to increased content of moisture. However, the degree of cure of the resin can be affected by the moisture and surfactants thus the ILSS trend cannot simply be based on the void content as the literature reported autoclave experiments. The ILSS of a CFRP laminate is affected by the following factors including the void content (negative effect), the exposure to moisture (positive effect for curing to a limit, negative effect to void content), the surfactants (negative effect for curing), and the CNF Z-thread (positive effect).

CHAPTER V

CONCLUSION

In this preliminary experimental study, the effect of CFRP and CNF z-threaded CFRP (i.e., ZT-CFRP) prepregs' moisture exposure prior the curing process was investigated by evaluating the cured composite laminate samples through the double notch shear (DNS) test, hardness test, and microscopy analysis. The prepreg's moisture exposure was done with RH-71.37% for 24 hours in an outdoor environment. The OOA-VBO curing cycle used in this study had a relative short debulking/degas duration of 10 minutes to only remove the excess air but not all the moisture in the prepreg stack prior curing. The post-cure was done at 180 degree C without vacuum for two hours rather than four hours so the final curing could show some difference due to moisture. The mild moisture exposure helped the curing of the resin and yielded 10.40% improvement of ILSS and produced the highest hardness. This is likely due to the small amount of water enhanced the curing rate and plasticized/toughened the resin. The ZT-CFRP without moisture exposure also showed a 10.36% increase in the ILSS due to the CNF z-threads providing the resistance/reinforcement against shear failure. However, it was found the ZT-CFRP composite samples had the lowest hardness values. It is possible that the added surfactants slightly slowed down the epoxy curing reaction and could require a longer post curing duration to be fully cured. The ZT-CFRP with moisture exposure samples showed 6.3% ILSS improvement against the control CFRP without moisture exposure. While one expects that the moisture would help the curing and CNF z-threads would also help the

ILSS, it could be disappointing that the ILSS of this set of ZT-CFRP prepreg with RH exposure did not produce the highest ILSS values among all four types of samples. It is possible that the room temperature dwelling stage (debulk/de-gas) which was merely 10 minutes, is too short compared with regular OOA-VBO practice of hours debulk/de-gas stage. From this observation, an additional ZT-CFRP prepreg exposed could be included laminate in the experiment to see the effect of one-hour debulking/degassing at room temperature and four-hours of post cure. The DNS evaluated sample produced lower ILSS among ZT-CFRP laminates and the hardness was one of the lower sides among all the samples. Moreover, the microscopic image (Figure 12) shows the big and randomly distributed 10.05% void fraction. The DNS test results of this extended test demonstrate the moisture effect and ILSS drop in the traditional CFRP and ZT-CFRP laminate (see Figure 15). The traditional CFRP laminates ILSS reduction due to void is sharp and becomes half when there is 8% void content present in the laminate, although, ZT-CFRP experience drop of ILSS as void increase. However, it dropped approximately 15% within a similar range of void present in the laminate.

Given that the CNF has a hollow tube structure, the excessive moisture could be trapped in the CNF and may not have been removed by the short debulk/degas process. The excessive moisture, as supported by the literatures can cause adverse effects on the ILSS, possibly due to voids and the inhibiting of the maximum achievable degree of cure near the water pockets. The moisture effect on the nanotechnology, especially given the hollow tube structure of nanofillers, could have complex implications for composite manufacturing as indicated in this study.

5.1 Future Works

In order to optimize the combined synergetic effects, one will need to find the near optimal OOA-VBO processing parameters and prepreg RH control conditions. For this experiment, the prepreg was exposed to outdoor RH on different days with an average 71% RH condition for 24 hours to compare the effect in real-life scenarios (like prepreg transportation with imperfect moisture control). The wind speed on those days was not in consideration which may create a difference in prepreg total amount of moisture absorption. Hence, control of the total environment in which prepreg gets exposed is important. In the extended work, someone might want to expose prepreg in a controlled environment like a RH control chamber which will ensure the absorption of an equal amount of moisture. If it is possible, the sample should be tested a week later from the date of laminate manufacture which will ensure that the laminates are fully cured in order to simulate a more realistic industrial practice. This will prevent the buckling phenomenon during the test observed during this experiment. The future work is reasonable based on our current knowledge. A question remains regarding how much moisture content is really encountered in the industrial manufacturing practice? That part of data may need to be considered as future work.

REFERENCES

1. P.K. Mallick, Fiber-Reinforced Composites. 3rd ed. Boca Raton, 2007. https://doi.org/10.1201/9781420005981
2. N. Sharp, C. Li, A. Strachan, D. Adams, R.B. Pipes, Effects of water on epoxy cure kinetics and glass transition temperature utilizing molecular dynamics simulations. 1st ed. Wiley Periodicals, Inc, 2017. https://doi.org/10.1002/polb.24357
3. Effect of water sorption on the structure and mechanical properties of ... (n.d.). Retrieved April 7, 2022. https://doi.org/10.1002/1097-4628(20010404)80:1<71::AID-APP1077>3.0.CO;2-H
4. M. Lettieri, M. Frigione, Effects of RH environment on thermal and mechanical properties of a cold-curing structural epoxy adhesive. Vol. 30. 2012. https://doi.org/10.1016/j.conbuildmat.2011.12.077
5. K.-T. Hsiao, A.M. Scruggs, J.S. Brewer Jr, G.J.S. Hickman, E.E. McDonald, K. Henderson, "Effect of carbon nanofiber z-threads on mode-I delamination toughness of carbon fiber reinforced plastic laminates." Composites Part A: Applied Science and Manufacturing, Volume 91, December 2016, 324–335. http://dx.doi.org/10.1016/j.compositesa.2016.10.022
6. S. Kirmse, B. Ranabhat, K-T Hsiao, Experimental and analytical investigation on the interlaminar shear strength of carbon fiber composites reinforced with carbon nanofiber z-threads, Materials Today Communications, Volume 25, December 2020, 101512.
7. B. Ranabhat, K.-T. Hsiao, "Improve the through-thickness electrical conductivity of CFRP laminate using flow-aligned carbon nanofiber z-threads." Proceedings of SAMPE 2018, Long Beach, CA, May 21-24, 2018.
8. M. Scruggs, S. Kirmse, and K.-T. Hsiao, "Enhancement of Through-Thickness Thermal Transport in Unidirectional Carbon Fiber Reinforced Plastic Laminates due to the Synergetic Role of Carbon Nanofiber Z-Threads." Journal of Nanomaterials, Volume 2019, Article ID 8928917, https://doi.org/10.1155/2019/8928917

9. Ahmad, H. “A Review of Carbon Fiber Materials in Automotive Industry.” IOP Conference Series: Materials Science and Engineering, vol. 971, no. 3, 2020, p. 032011., https://doi.org/10.1088/1757-899x/971/3/032011.

10. Ahmad, Jamal. “Machining of Polymer Composites.” 2009, https://doi.org/10.1007/978-0-387-68619-6

11. “Sports Composites Market Size Worth $4.58 Billion by 2024.” Market Research Reports & Consulting, https://www.grandviewresearch.com/press-release/global-sports-composites-market.

12. Sebastian Kirmse, “ZT-CFRP technology: A high-performance and comprehensive alternative to conventional CFRPs Reinforced Plastics” Volume 65, Issue 5, 2021, https://doi.org/10.1016/S0034-3617(21)00263-0.

13. “Effects of Material and Process Parameters on Void Evolution in Unidirectional Prepreg during Vacuum Bag-Only Cure.” Journal of Composite Materials, vol. 54, no. 5, 2019, pp. 633–645., https://doi.org/10.1177/0021998319864420.

14. T. Ozkan, M. Naraghi, I. Chasiotis, Mechanical properties of vapor grown carbon nanofibers, Carbon 48 (2009) 239–244

15. Kuang-Ting Hsiao and Gregory Hickman, “Method for manufacturing nano-structurally aligned multi-scale composites”, US10066065B2, 2020-6-24 https://patents.google.com/patent/US10066065B2

16. ASTM D3846-02, Standard Test Method for In-Plane Shear Strength of Reinforced Plastics, ASTM International, West Conshohocken, PA, 2015, www.astm.org

17. ASTM D792-13, Standard Test Methods for Density and Specific Gravity (Relative Density) of Plastics by Displacement, ASTM International, West Conshohocken, PA,2013, www.astm.org

18. “Standard Test Method for Compressive Properties of Rigid Plastics.” ASTM International - Standards Worldwide, https://www.astm.org/d0695-02.html.

BIOGRAPHICAL SKETCH

Name of Author: Md Nazim Uddin

Graduate and Undergraduate Schools Attended:

The University of South Alabama, Mobile, Alabama

Degrees Awarded:

Bachelor of Science in Mechanical Engineering (BSME) 2020
Master of Science in Mechanical Engineering (MSME) 2022

Awards and Honors:

Graduate Research Assistant, Dean’s listed, Member of Tau Beta Pi Honor society.